Research Article | Vol. 25, No. 22 | 30 Oct 2017 | OPTICS EXPRESS 27464
Optics EXPRESS

Direct experimental measurement of single-mode and mode-hopping dynamics in frequency swept lasers

T.P. BUTLER,[1,2,4,*] D. GOULDING,[1,2] B. KELLEHER,[2,3] B. O'SHAUGHNESSY,[1,2] S. SLEPNEVA,[1,2] S.P. HEGARTY[1,2] AND G. HUYET[1,2,5,6]

[1]*Center for Applied Photonics and Process Analysis, Department of Physical Sciences, Cork Institute of Technology, Ireland*
[2]*Tyndall National Institute, University College Cork, Ireland*
[3]*Department of Physics, University College Cork, Ireland*
[4]*Max Planck Institute of Quantum Optics, Hans-Kopfermann-Str. 1, 85748 Garching, Germany*
[5]*Université Côte d'Azur, CNRS, Institut de Physique de Nice, F-06560 Valbonne, France*
[6]*National Research University of Information Technologies, Mechanics and Optics, Saint Petersburg, Russia*
[*]*thomas.butler@mpq.mpg.de*
www.cappa.ie

Abstract: A time-resolved study is presented of the single-mode and mode-switching dynamics observed in swept source vertical cavity surfing emitting lasers and swept wavelength short external cavity lasers. A self-delayed interferometric technique is used to experimentally measure the phase and intensity of these frequency swept lasers, allowing direct examination of the modal dynamics. Visualisation of the instantaneous optical spectrum reveals mode-hop free single mode lasing in the case of the vertical cavity laser, with a tuning rate of 6.3 GHz/ns. More complex mode-switching behaviour occurs in the external cavity laser, with the mode-hopping dynamics found to be dominated by the deterministic movement of the spectral filter. Evidence of transient multi-mode operation and mode-pulling is also presented.

OCIS codes: (140.3600) Lasers, tunable; (120.5050) Phase measurement.

References and links

1. G. R. Gray and R. Roy, "Bistability and mode hopping in a semiconductor laser," J. Opt. Soc. Am. B **8**(3), 632–638 (1991).
2. M. Ohtsu and Y. Teramachi, "Analyses of mode partition and mode hopping in semiconductor lasers," IEEE J. Quant. Electron. **25**, 31–38 (1989).
3. D. Lenstra, B. H. Verbeek and A. J. Den Boef, "Coherence collapse in single-mode semiconductor lasers due to optical feedback," IEEE J. Quant. Electron. **21**, 674–679 (1985).
4. T.B. Simpson, J.M. Liu, A. Gavrielides, V. Kovanis and M. Alsing, "Period-doubling route to chaos in a semiconductor laser subject to optical injection," Appl. Phys. Lett. **64**, 3539 (1994).
5. D. Goulding, S. P. Hegarty, O. Rasskazov, S. Melnik, M. Hartnett, G. Greene, J. G. McInerney, D. Rachinskii and G. Huyet, "Excitability in a quantum dot semiconductor laser with optical injection," Phys. Rev. Lett. **98**, 153903 (2007).
6. N. Chinone, T. Kuroda, T. Ohtoshi, T. Takahashi and T. Kajimura, "Mode-hopping noise in index-guided semiconductor lasers and its reduction by saturable absorbers," IEEE J. Quantum Electron. **21**(8), 1267–1270 (1985).
7. O. Lux, S. Sarang, R. J. Williams, A. McKay and R. P. Mildren, "Single longitudinal mode diamond Raman laser in the eye-safe spectral region for water vapor detection," Opt. Express **24**(24), 27812–27820 (2016).
8. M. Ohtsu, Y. Otsuka and Y. Teramachi, "Precise measurements and computer simulations of mode-hopping phenomena in semiconductor lasers," Appl. Phys. Lett. **46**(2), 108–110 (1985).
9. M. Ohtsu, Y. Teramachi, Y. Otsuka and A. Osaki, "Analyses of mode-hopping phenomena in an AlGaAs laser," IEEE J. Quantum Electron. **22**(4), 535–543 (1986).
10. L. Furfaro, F. Pedaci, M. Giudici, X. Hachair, J. Tredicce and S. Balle, "Mode-switching in semiconductor lasers," IEEE J. Quantum Electron. **40**(10), 1365 (2004).
11. L. Furfaro, F. Pedaci, J. Javaloyes, X. Hachair, M. Giudici, S. Balle and J. Tredicce, "Modal switching in quantum-well semiconductor lasers with weak optical feedback," IEEE J. Quantum Electron. **41**(5), 609–618 (2005).

#303926 https://doi.org/10.1364/OE.25.027464
Journal © 2017 Received 7 Aug 2017; revised 14 Sep 2017; accepted 14 Sep 2017; published 24 Oct 2017

Optics EXPRESS

12. S. H. Yun, "Mode locking of a wavelength-swept laser," Opt. Lett. **30**(19), 2660–2662 (2005).
13. E. Avrutin and L. Zhang, "Dynamics of semiconductor lasers under fast intracavity frequency sweeping," IEEE 14th International Conference on Transparent Optical Networks (ICTON) (2012), pp. 1–4.
14. S. Slepneva, B. Kelleher, B. O'Shaughnessy, S. P. Hegarty, A. Vladimirov and G. Huyet, "Dynamics of Fourier domain mode-locked lasers," Opt. Express **21**(16), 19240–19251 (2013).
15. S. Slepneva, B. O'Shaughnessy, B. Kelleher, S. P. Hegarty, A. Vladimirov, H.-C. Lyu, K. Karnowski, M. Wojtkowski and G. Huyet, "Dynamics of a short cavity swept source OCT laser," Opt. Express **22**(15), 18177–18185 (2014).
16. S. R. Chinn, E. A. Swanson and J. G. Fujimoto, "Optical coherence tomography using a frequency-tunable optical source," Opt. Lett. **22**(5), 340–342 (1997).
17. F. Lexer, C. Hitzenberger, A. Fercher and M. Kulhavy, "Wavelength-tuning interferometry of intraocular distances," Appl. Opt. **36**(25), 6548–6553 (1997).
18. B. Golubovic, B. Bouma, G. Tearney and J. Fujimoto, "Optical frequency-domain reflectometry using rapid wavelength tuning of a Cr^{4+}:forsterite laser," Opt. Lett. **22**(22), 1704–1706 (1997).
19. R. Passy, N. Gisin, J. P. von der Weid and H. H. Gilgen, "Experimental and theoretical investigations of coherent OFDR with semiconductor laser sources," J. Lightwave Technol. **12**(9), 1622–1630 (1994).
20. J. A. Izatt and M. A. Choma, "Theory of optical coherence tomography," in Optical Coherence Tomography, W. Drexler and J. G. Fujimoto, eds. (Springer International Publishing, 2008), pp. 47–72.
21. R. Huber, M. Wojtkowski and J. Fujimoto, "Fourier domain mode locking (FDML): A new laser operating regime and applications for optical coherence tomography," Opt. Express **14**(8), 3225–3237 (2006).
22. M. Kuznetsov, W. Atia, B. Johnson, and D. Flanders, "Compact ultrafast reflective Fabry-Pérot tunable lasers for OCT imaging applications," Proc. SPIE, **7554**, 75541F (2010).
23. S. Gloor, A. H. Bachmann, M. Epitaux, T. von Niederhausern, P. Vorreau, N. Matuschek, K. Hsu, M. Duelk and C. Velez, "High-speed miniaturized swept sources based on resonant MEMS mirrors and diffraction gratings," Proc. SPIE **8571**, 85712X (2013).
24. I. Grulkowski, J. Liu, B. Potsaid, V. Jayaraman, C. Lu, J. Jiang, A. Cable, J. Duker and J. Fujimoto, "Retinal, anterior segment and full eye imaging using ultrahigh speed swept source OCT with vertical-cavity surface emitting lasers," Biomed. Opt. Express **3**(11), 2733–2751 (2012).
25. T. Butler, S. Slepneva, B. O'Shaughnessy, B. Kelleher, D. Goulding, S. P. Hegarty, H.-C. Lyu, K. Karnowski, M. Wojtkowski, and G. Huyet, "Single shot, time-resolved measurement of the coherence properties of OCT swept source lasers," Opt. Lett. **40**(10), 2277–2280 (2015).
26. D. Goulding, T. Butler, B. Kelleher, S. Slepneva, S. P. Hegarty and G. Huyet, "Visualisation of the phase and intensity dynamics of semiconductor lasers via electric field reconstruction," in *Nonlinear Dynamics: Materials, Theory and Experiments*, M. Tlidi and M. G. Clerc, eds. (Springer 2016), pp. 3–30.
27. B. Kelleher, D. Goulding, B. Baselga Pascual, S.P. Hegarty and G. Huyet, "Phasor plots in optical injection experiments," Eur. Phys. J. D **58**(2), 175–179 (2010).
28. F. Gustave, L. Columbo, G. Tissoni, M. Brambilla, F. Prati, B. Kelleher, B. Tykalewicz, and S. Barland, "Dissipative phase solitons in semiconductor lasers," Phys. Rev. Lett. **115**(4), 043902 (2015).
29. I. Grulkowski, J. J. Liu, B. Potsaid, V. Jayaraman, J. Jiang, J. G. Fujimoto and A. E. Cable, "High-precision, high-accuracy ultralong-range swept-source optical coherence tomography using vertical cavity surface emitting laser light source," Opt. Lett. **38**(5), 637–675 (2013).
30. S. Todor, B. Biedermann, W. Wieser, R. Huber and C. Jiruaschek, "Instantaneous lineshape analysis of Fourier domain mode-locked lasers," Opt. Express **19**(9), 8802–8807 (2011).

1. Introduction

Semiconductor lasers are a class of physical systems which display a host of dynamic behaviours. Non-linear dynamic effects in lasers have been studied extensively, both from the perspective of the underlying fundamental physics, in addition to how these dynamics affect laser performance and applications. Non-linear interactions lead to the existence of multiple dynamic phenomena such as mode-hopping [1], mode partition [2], coherence collapse [3], deterministic chaos [4], and excitability [5]. These dynamics can occur under a variety of operating conditions, including free-running, operating under optical feedback, or subject to optical injection. Mode-hopping in particular is a dynamic regime which can have significant implications for single-mode laser applications [6], for example in the measurement of absorption spectra [7].

Mode-hopping, or mode-switching, is a dynamic regime in semiconductor laser systems which has been the focus of much study. Typically, mode-hopping dynamics are characterised by a time averaged multi-mode output. At any instant however, the emission of the laser is dominated by a single mode, with the dominant output switching between a number of supported

Optics EXPRESS

modes. While the temporal intensity may appear to be constant, with a single-mode output at all times, the switching dynamics can present problems in application settings. Often, the driving force behind mode-hopping events stems from the laser's amplified spontaneous emission noise [8, 9]. While noise-driven processes are common, deterministic mode-switching has also been observed [10,11]. In each case, robust time-resolved experimental characterisation of these dynamic systems is important in determining the actual behaviour.

Recently, swept frequency lasers have been shown to exhibit interesting non-linear dynamics [12–15]. Swept frequency lasers differ from conventional single-mode or quasi-tunable lasers by introducing a fast tunable intra-cavity spectral filter. Often used in imaging and interferometric sensing applications (for example optical coherence tomography, OCT [16–18], or optical frequency domain reflectometry, OFDR [19]), swept lasers are designed to produce a wide-bandwidth, periodic, low linewidth, and continuous tuning output [20]. Semiconductor-based devices are employed in many commercially available swept source engines, including Fourier domain mode-locked lasers [21], short external cavity based lasers [22, 23], and vertical cavity surface emitting lasers [24]. With a constantly changing intra-cavity spectral filter, the dynamics observed in these systems are now found to be dependant on the filter speed and direction, as well as how the filter transmission band interacts with the gain bandwidth of the semiconductor. The study of these dynamics informs many of the design considerations for new devices with increased imaging effectiveness.

Recently, the authors have demonstrated a novel method of characterising swept frequency lasers. Using a self-delayed heterodyne approach, it is possible to reconstruct the complex electric field of a swept source laser and therefore examine many aspects of the laser, including the temporal, spectral and coherence properties [25]. Previous work has detailed applying this method to the measurement of the instantaneous linewidth and coherence roll-off, two important benchmarks of a swept source in OCT imaging. This work utilises the same 3×3 interferometric technique [26], this time focussing on resolving the temporal phase dynamics of two swept sources and investigating the observed single-mode and mode-hopping behaviours. This characterisation technique allows for single-shot, high time resolution measurement of the instantaneous spectrum of swept sources, enabling direct visualisation of laser dynamics.

2. Experimental technique

The experimental set-up of the 3×3 self-delayed heterodyne technique is the same as presented in [25]. The procedure utilises a 120° optical hybrid fibre coupler with 3 inputs and outputs. The swept source signal is split into two equal parts and a short time delay applied to one of the signals. Upon mixing the signal and its delayed version using two inputs of the 3×3 coupler, the heterodyne beat signals which are produced can be combined to provide a measurement of the original laser phase, $\phi(t)$. Parallel to the phase measurement interferometer, the instantaneous intensity, $I(t)$, is simultaneously measured, allowing for recovery of the total electric field, $E(t) = \sqrt{I(t)}\exp(i\phi(t))$. A similar technique has been applied to the study of the dynamics of optically injected semiconductor lasers [27] and semiconductor laser solitons [28]. By using a real-time oscilloscope and high speed photodetectors in the detection of the beat signals, the electric field can be reconstructed with a temporal resolution set by the sampling speed of the oscilloscope (25 ps), and a temporal span only limited by its memory depth (250 μs). The primary limitation of the reconstruction of the electric field is that the instantaneous spectral width of the laser under test must remain smaller than the effective detection bandwidth, in this case approximately 12 GHz. In practice, this limitation is acceptable for many swept source lasers. This self referenced approach to the measurement further means that there is no limitation on the total sweep bandwidth of the laser. Sweeps as wide as 100 nm (~20 THz) have been characterised in a single shot using this method.

Optics EXPRESS

3. Swept vertical cavity surface emitting laser

In order to demonstrate the power of the electric field reconstruction technique, a relatively simple laser field was first examined. In this case, a swept VCSEL provides a fast tuning single mode output. The VCSEL device is a commercially available OCT engine (Thorlabs Inc.) based on a micro-electro-mechanical systems (MEMS) tuning mechanism [29]. The upper Bragg reflector is grown on top of a MEMS membrane, allowing for fast tuning of the cavity length of the laser. Because of the micro-cavity length and subsequent large free spectral range, only a single axial mode can exist in the gain region at any one time. By altering the cavity length the position of this single mode changes, producing a mode-hop free fast tuning output. The laser operates at 1300 nm with a full sweep width of over 100 nm, and a repetition rate of 200 kHz (5 μs period).

Figure 1 illustrates the acquired electric field information. The upper inset plot shows the recovered instantaneous frequency over the course of a single sweep period. The main part of the sweep used during imaging is the positive frequency sweep direction, which is approximately 3 μs long. The laser is switched off for the return sweep, meaning reconstruction of the phase is impossible during the other 2 μs of the sweep. The instantaneous frequency is useful for examining the overall macro-behaviour of the laser output, however, interpretation of the single-valued function can be difficult if complex dynamics or multiple modes are present. A more physically intuitive visualisation of the field can be obtained by calculating the time-resolved instantaneous optical spectrum of the laser. A windowing function is utilised in order to perform this calculation. Windowing the electric field allows examination of short field sections independent of the rest of the signal. A Hanning window is used in this work. The Hanning function, $\mathcal{H}(t,\tau)$ is defined by the center position of the window, τ, as well as the length of the window, δt, which is fixed in this work at 2.5 ns. Multiplying the window function by the reconstructed electric field, $E(t)$, the two-dimensional instantaneous optical spectrogram can be computed using the fast Fourier transform, via

$$S(\omega,\tau) = \left|\mathrm{FFT}\left[\mathcal{H}(t,\tau)E(t)\right]\right|^2, \tag{1}$$

where S is the power spectral density, ω is the frequency of the signal, and FFT[f(t)] represents the fast Fourier transform of a signal $f(t)$.

The main plot of Fig. 1 shows the calculated spectrogram of the electric field of the VCSEL laser over a 30 ns region. In order to avoid wrapping of the wide sweep to the 40 GHz nyquist bandwidth, the recovered complex electric field is linearly interpolated to a smaller sampling period, thereby allowing visualisation of the sweep over the entire 200 GHz shown in Fig. 1. Mode-hop free, chirped single-mode emission is observed, with a sweep rate of approximately 6.3 GHz/ns. As expected for the VCSEL design, there is no evidence of any other lasing modes or a modulated intensity. This single-mode behaviour is similarly observed across the entire 3 μs negative sweep. The lower subplot shows another measurement made possible by full knowledge of the electric field. By accounting for the constant chirp of the laser field, the average instantaneous lineshape of the single mode can be recovered. The instantanoues linewidth of the laser can be decoupled from the shift of the MEMS tuning by removing the associated linear chirp from the measured frequency function and calculating the power spectral density of the now stationary field. The average linewidth in this case is approximately 225 MHz. Compared to several other swept sources, this linewidth is significantly lower [25, 30].

4. Swept external cavity laser

Reconstruction of the vertical cavity laser electric field is instructive in understanding the capability of the experimental technique in producing optical spectrograms. However, the dynamics of the VCSEL laser emission are quite simple. Other swept sources showing much more com-

Optics EXPRESS

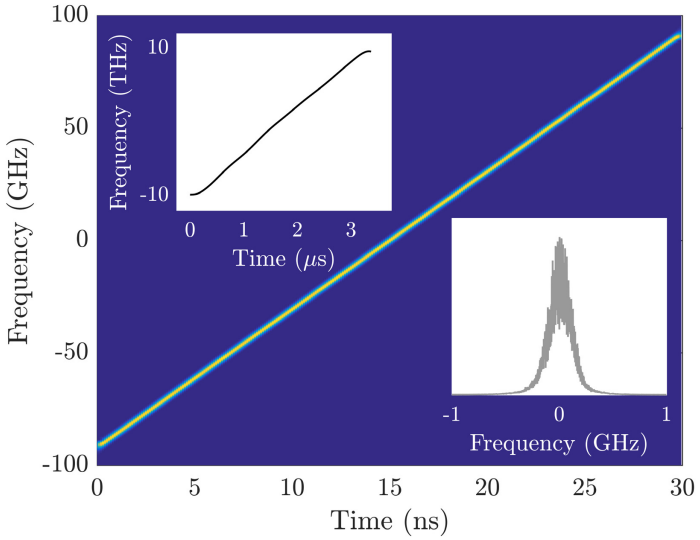

Fig. 1. Electric field reconstruction of a swept VCSEL. The main plot shows the electric field spectrogram of a short section in the middle of the sweep, showing mode-hop free single mode emission. The upper inset presents the instantaneous frequency recovered for the entire forward sweep. The lower inset presents the average instantanteous lineshape of the laser, with a linewidth of ~225 MHz.

plex dynamics are less easily understood using conventional optical spectrum analysis or heterodyne measurements. Using the novel 3×3 analysis however, the underlying cavity dynamics can be investigated.

One laser that shows multiple different dynamic regions is the short cavity swept source laser. This laser utilises an external cavity geometry, with the spectral filtering element generally being provided by a MEMS based mirror, filter, or grating arrangement. The device used in this work is a commercially available short cavity swept source produced by AXSUN Technologies Inc. [22]. It utilises a MEMS based multi-mode Fabry-Pérot filter which acts as both a cavity reflector and a tunable filter, along with a semiconductor optical amplifier (SOA) gain region. With a central wavelength of 1310 nm, the laser sweep is approximately 100 nm wide with a repetition rate of 50 kHz. The operation of the laser while sweeping differs significantly from the vertical cavity laser presented previously. Because the length of the cavity is on the order of 10 cm, the resonator is able to support a large number of external cavity modes, defined by the cavity length. Examining the electronic power spectrum of the laser, the fundamental mode spacing is determined to be ~1.33 GHz. As the central position of the intra-cavity filter changes, a small portion of the available modes will lase at any one time. The exact behaviour of the laser depends on the filter speed, direction, and SOA non-linearities. Previous studies of this laser have identified quasi-cw, pulsing, and complex intensity outputs using experimental and theoretical modelling [15].

Figure 2 presents the results of the electric field reconstruction of the swept external cavity laser. Figure 2(a) shows the recovered instantaneous wavelength over the course of two complete sweeps. The sweep is asymmetric, with approximately 12 μs in the forward sweep (positive wavelength direction) and 8 μs in the backward sweep. This work will focus on the extrema of the sweep, as highlighted with the box. During both the top and bottom of the sweep, the filter is moving relatively slowly, as it reaches the end of the sweep and stops to return to its original position. During this time, the output of the laser is observed to contain regions of

Optics EXPRESS

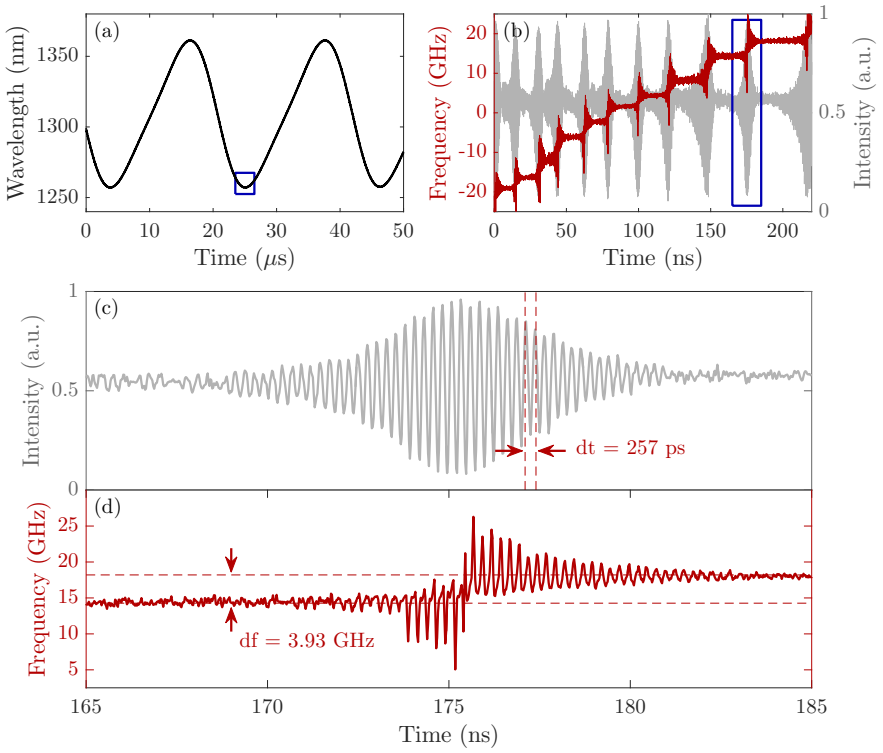

Fig. 2. (a) Recovered single shot instantaneous frequency of the short cavity laser over a 50 μs measurement. (b) Time-resolved intensity (grey) and frequency (red) of the laser during the slow part of the filter path. (c) Intensity and (d) frequency of the laser during a single mode hopping event, as indicated by the box in (b).

CW output interrupted by oscillating intensity transients. An example of a representative intensity trace can be seen in Figure 2(b). This figure also presents the associated instantaneous frequency. It is clear from the phase measurement that during the CW output times, the laser frequency remains relatively constant, with more complex dynamics occurring along with the transient intensity oscillations. The behaviour during this region seems consistent with multiple mode-hopping events; the lasing modes are changing in order to keep up with the movement of the filter bandpass. Figure 2(c) and Fig. 2(d) show a zoom of the intensity and frequency of the laser during one such mode-hopping event. The periodic nature of the intensity transient implies that it is formed by the beating of two discrete frequencies. Comparing the change in frequency of the laser before and after the transient (3.93 GHz) to the period of the transient (257 ps), the measurement suggests that the oscillation is formed from the beating of two independent cavity modes, separated by three times the cavity fundamental repetition rate.

The dynamics seen in Fig. 2 can be explained by a very simple mode-hopping mechanism. While stationary, or slowly moving, the laser output is dominated by single-mode emission. As the filter bandpass moves further away from the dominant mode, however, this mode suffers additional loss. At a certain point, the center of the filter is far enough away from the lasing mode that it is no longer at the preferred operating point. The oscillating transients mark the extinction of the lasing mode as it is attenuated, and a new mode begins to lase. This new mode, which is closer to the center of the filter, is seeded by amplified spontaneous emission from

Optics EXPRESS

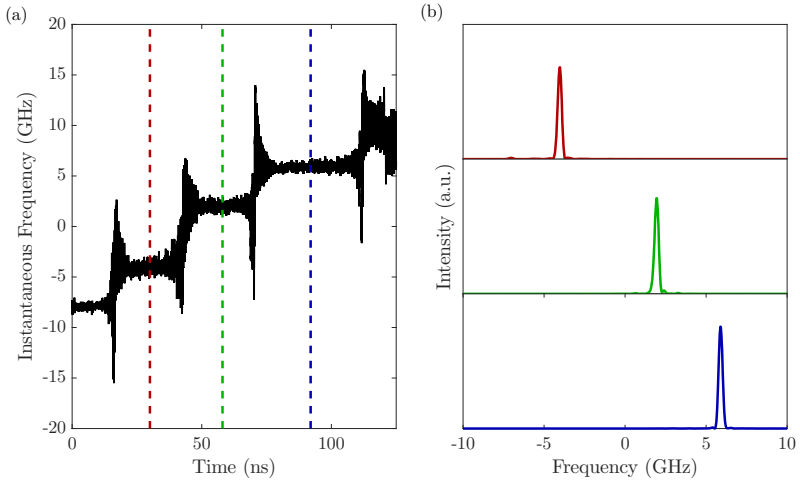

Fig. 3. (a) Instantaneous frequency during a mode-hopping event. (b) Instantaneous optical spectra corresponding to the three dashed lines in (a) showing the laser spectrum during the CW regions. See Visualisation 1 for an animation of this measurement.

the SOA. A more complete view of this dynamic regime can be accessed by calculating the instantaneous optical spectrum. As with the VCSEL, the electric field is windowed and at each center time, the optical spectrum during a 2.5 ns segment is computed. Figure 3 shows several experimentally recovered, single shot measurements of the laser spectrum during the flat part of the frequency steps. Between each transient event, and corresponding to the CW-like output intensity regions, the laser operates in a single frequency mode. The linewidth of each mode can be determined by spectral filtering of the recovered field. The average linewidth of the single mode sections is approximately 400 MHz, larger than that of the vertical cavity laser.

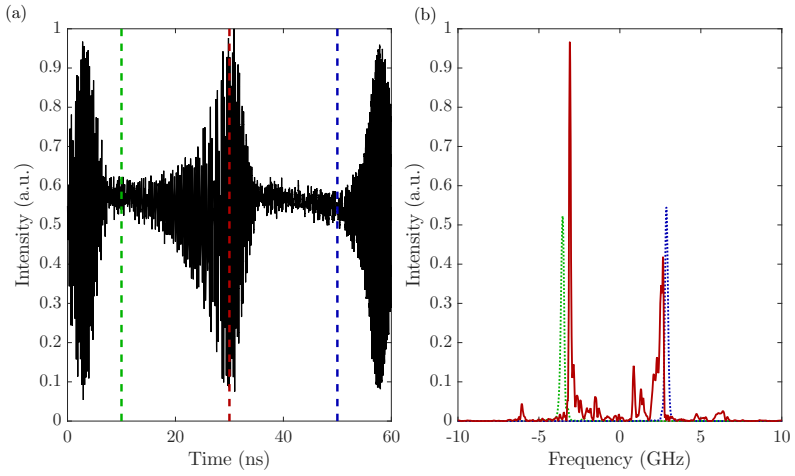

Fig. 4. (a) Time resolved intensity during a mode-hopping event. (b) Instantaneous optical spectra corresponding to the three dashed lines in (a) showing the laser spectrum before, during and after the mode-hopping event.

Figure 4 displays a similar set of optical spectra, this time focussing on the evolution of the

spectrum before, during and after the transient oscillation. As in Fig. 3, before and after the transient the laser operates at a single frequency. During the center of the transient however, multiple emission frequencies are observed. As expected from the acquired time-traces, the output is dominated by the simultaneous lasing of the two dominant modes, namely the initial and final modes involved in the mode-hop. The instantaneous optical spectrum further reveals two details of the mode-hopping phenomenon that were not previously visible. Figure 4(b) shows that during the transient, there is energy present in several nearby modes, adjacent to both the initial and final modes. The figure also shows some evidence of mode-pulling, which is measured in more detail later in this work.

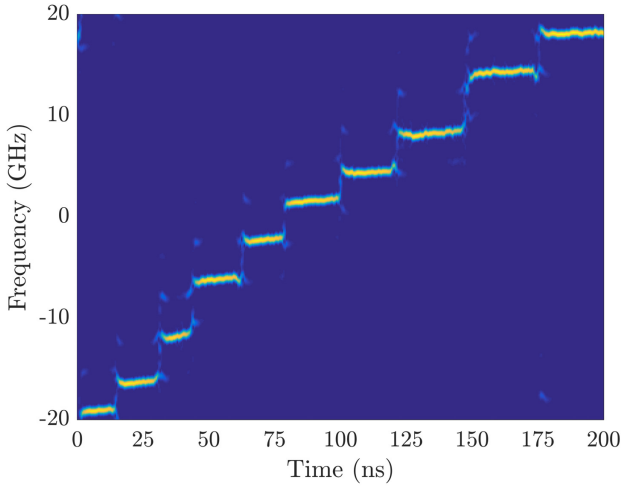

Fig. 5. Optical spectrogram of the mode-hopping occuring in the AXSUN laser.

The time-resolved optical spectra can be displayed concurrently as a spectrogram, detailing the laser dynamics during multiple mode-hopping events. Figure 5 presents the calculated optical spectrogram during a 200 ns region of mode-hopping emission. This view of the electric field confirms the presence of multiple modes during the transient oscillations, with sharp single mode emissions in-between. The overall output of the laser follows the centre position of the filter bandpass. However, unlike in the case of the VCSEL, the laser's centre frequency remains fixed over as long a period as possible until the motion of the filter places the dominant mode in a position where it can no longer acquire sufficient gain. At this point the laser must mode-hop to a more favourable mode, where it can continue emitting in a single-mode.

The optical spectrogram also confirms the presence of significant mode-pulling occurring as the laser approaches and recovers from the transient regime. Figure 6 shows the extent of this pulling measured for the nine complete modes shown in the spectrogram of Fig. 5. The relative centre frequency of each mode is tracked during its lifetime, and presented together with a fixed offset to differentiate the different modes. Each of the modes has a small positive chirp, with the frequency changing on average +29.5 MHz/ns during the mode-lifetime. Towards the beginning and end of each mode, however, there is a much more significant change in the mode's centre frequency, with an average deviation of approximately 430 MHz due to this mode-pulling behaviour. Mode-pulling and mode-chirp are both caused by the non-linear nature of the semiconductor amplifier, as well as the effect of the filter on the phase of the circulating field in the cavity.

Optics EXPRESS

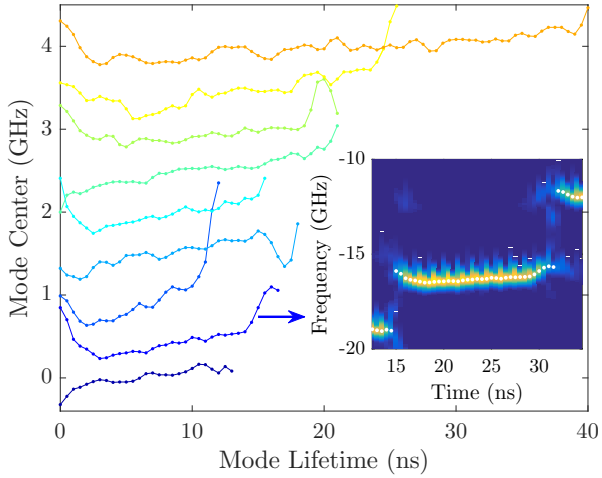

Fig. 6. Center frequency of each of the modes presented in Fig. 5 over their relative lifetimes. Inset shows the measured centres for a single mode plotted over the spectrogram. Each mode is measured from its relative creation time. The frequency axis is relative, with a fixed offset (0.5 GHz) between each line used to make the behaviour of each mode clear.

5. Mode-hopping statistics

With access to the electric field in a time-resolved, single-shot format, it becomes possible to examine the longer time scale behaviour of the mode-hopping regime, rather than single or short groups of events. Two such measurements of interest in this case are the mode lifetimes, Δt, and mode spacing, Δf, of the mode-hopping in the swept frequency laser. Visualisation of these parameters enables a better understanding and confirmation of the underlying physics driving the mode-hopping transitions.

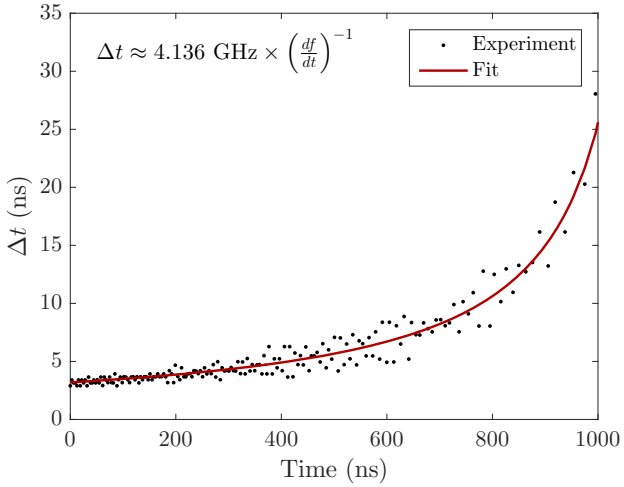

Fig. 7. Experimentally measured mode lifetime during a 1 μs section of mode-hopping. During this time the filter speed is slowing down. The line plots a fit to the lifetime in terms of the linearly decreasing filter speed.

Optics EXPRESS

In many mode-hopping systems, the driving force stems from the stochastic effect of the ASE noise present in the laser cavity. This noise-driven process means that the lifetime of any one mode cannot generally be predicted [8]. In the case of the swept frequency laser, however, it is expected that the destabilising nature of the moving spectral filter will be a much more influential factor in the dynamics that occur. If the mode-hopping process occurs as discussed previously, it is clear that the lifetime of each mode should be dependant on the amount of time that the filter remains near the dominant mode before forcing the mode-hop. Figure 7 presents the measured mode lifetimes over a 1000 ns section of the sweep. This part of the sweep occurs just before the maximum of the frequency span, with the filter stopping and changing direction just after 1 μs. It is found that the lifetime of the modes increases as the filter moves towards the maximum point. Near these turning points in the filter sweep, the position of the filter can be well approximated by a second order polynomial, implying that during this time the filter speed is decreasing linearly toward zero, when the filter will change direction. The measured lifetimes can be compared to the fit line, which is inversely proportional to the filter speed, expressed in GHz/ns. It is clear that in this case there is good agreement between the measured values of the lifetime and the deterministic approximation. Physically, this means that as the filter movement slows, the dwell time around a particular mode becomes larger, allowing that mode to lase freely for a longer time before another transient occurs.

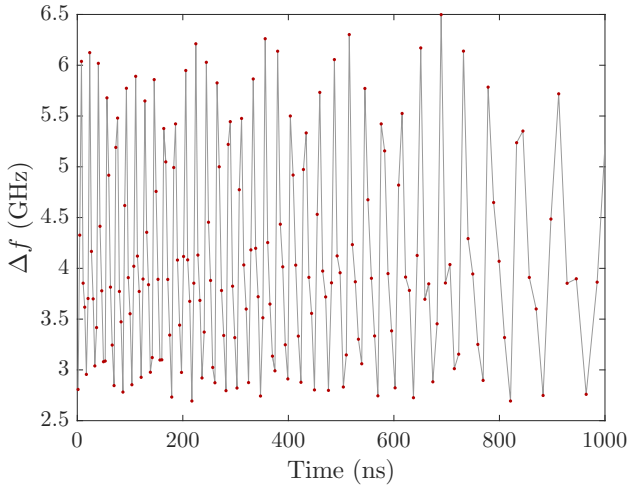

Fig. 8. Frequency spacing evolution between adjacent mode hops during 1 μs of lasing.

Along with the lifetime of each mode, the central frequency of each mode can also be measured from the recovered electric field. The frequency difference, or mode spacing, Δf, is another measurement that sheds light on the nature of the mode-hopping regime. A first order approximation of the sliding frequency mode-hopping would assume that while the lifetime is dependant on the filter speed, the mode spacing should be constant. As one mode is attenuated by the filter tail, a new mode is chosen closer to the center of the filter, a fixed frequency Δf each time. However, this view neglects factors such as mode competition, gain saturation, and seeding by ASE, which may make the changes more complicated or even stochastic in nature. Figure 8 plots the experimentally measured mode spacing for the same time period as the previous figure. It is clear that the mode spacing is neither constant nor random, with a clear structure observed. The mode spacing oscillates between large (approximately 5 fundamental cavity modes) and small (approximately 2 fundamental cavity modes) spacings. The mode spacing is not strictly periodic in time, due to the changing lifetimes discussed in Fig. 7. It is found, however, that

Optics EXPRESS

there are either 5 or 6 mode hops occurring in each cyclic event observed in the mode spacing, as shown in Fig. 8. Grouping the modes together in a single period, it is observed that each group of modes spans approximately 20 GHz bandwidth. That is, every 20 GHz that the filter moves in the frequency domain, the mode-hopping transition spacings reset and begin to repeat. Once again, this measurement shows that the mode-hopping regime of the swept frequency external cavity laser is largely a deterministic process, driven by the movement of the intra-cavity spectral filter.

6. Conclusion

This work has presented a detailed examination of the electric field dynamics of two commercially available swept source lasers, based on semiconductor VCSEL and external cavity configurations. Self-delayed heterodyne measurements of the lasers under test allow for time-resolved, single-shot reconstructions of the complex electric field to be made. These phase resolved experimental measurements capture the electric field with a 25 ps time resolution over the entire wide bandwidth (~20 THz) sweep. This work focussed on the single-mode and mode-hopping dynamics observed in these lasers. Real-time electric field measurements enable time-resolved study of the lasers' instantaneous intensity, frequency, and optical spectrum. Reconstruction of the VCSEL laser shows mode-hop free, linearly chirped single-mode operation across the entire sweep, with a low single mode linewidth. In the external cavity swept source, slow movement of the intra-cavity filter leads to highly structured deterministic mode-hopping dynamics. Multi-mode transient operation was resolved in between the single-mode sections, forming transient intensity oscillations between the quasi-CW single-mode regions. This work highlights the power of the 3×3 interferometric field reconstruction technique in uncovering the fundamental behaviour of swept frequency light sources, presenting the clearest current picture of the temporal dynamics of swept sources.

Funding

Science Foundation Ireland (SFI) (11/PI/1152 and IPIC 12/RC/2276); European Union (EU) FP7 Marie Curie Action FP7-PEOPLE-2010-ITN through the PROPHET project (264687).